



HAL
open science

What Triggers Epitaxial Growth of GaN on Graphene?

Camille Barbier, Ludovic Largeau, Noëlle Gogneau, Laurent Travers,
Christophe David, Ali Madouri, Dyhia Tamsaout, Jean-Christophe Girard,
Guillemin Rodary, Hervé Montigaud, et al.

► **To cite this version:**

Camille Barbier, Ludovic Largeau, Noëlle Gogneau, Laurent Travers, Christophe David, et al.. What Triggers Epitaxial Growth of GaN on Graphene?. *Crystal Growth & Design*, 2023, 23 (9), pp.6517-6525. 10.1021/acs.cgd.3c00481 . hal-04173825

HAL Id: hal-04173825

<https://hal.science/hal-04173825v1>

Submitted on 17 Oct 2023

HAL is a multi-disciplinary open access archive for the deposit and dissemination of scientific research documents, whether they are published or not. The documents may come from teaching and research institutions in France or abroad, or from public or private research centers.

L'archive ouverte pluridisciplinaire **HAL**, est destinée au dépôt et à la diffusion de documents scientifiques de niveau recherche, publiés ou non, émanant des établissements d'enseignement et de recherche français ou étrangers, des laboratoires publics ou privés.

What triggers epitaxial growth of GaN on graphene?

*Camille Barbier, Ludovic Largeau, Noëlle Gogneau, Laurent Travers, Christophe David, Ali Madouri, Dyhia Tamsaout, Jean-Christophe Girard, Guillemin Rodary, Hervé Montigaud†, Christophe Durand‡, Maria Tchernycheva, Frank Glas, Jean-Christophe Harmand**

Centre de Nanosciences et de Nanotechnologies (C2N), Université Paris-Saclay, CNRS, 10 Bd
Thomas Gobert, 91120 Palaiseau, France

‡ Université Grenoble Alpes, CEA, Grenoble INP, IRIG, PHELIQS, NPSC, 17 avenue des
Martyrs, 38000 Grenoble, France

† Surface du Verre & Interfaces, UMR 125 CNRS/Saint Gobain recherche, 39 quai Lucien
Lefranc, BP 135, 93303 Aubervilliers, France

KEYWORDS : GaN, nanowire, epitaxy, graphene, nucleation, incubation, plasma

ABSTRACT: With the perspective of using two-dimensional materials as growth substrates for semiconductors, we explore the nucleation of GaN nanostructures on graphene. Using plasma-assisted molecular beam epitaxy, we investigate what happens during the long incubation time which precedes the epitaxy of the first GaN islands. After 30 min of nitrogen plasma exposure with no deposition, we find that graphene is modified and we identify C-N bonds. We measure and model the variation of the incubation time with the growth parameters. These data support the idea that graphene must be modified before GaN nucleation becomes possible. We then test the adhesion at the interface between graphene and the GaN nanostructures. Our studies converge on the conclusion that GaN nanostructures nucleate on graphene from pyridinic-N

atoms incorporated in the lattice, which are responsible for strong binding between the two materials.

Introduction

The use of a two-dimensional (2D) material as a substrate for epitaxial growth is a very attractive concept. Indeed, generally epitaxy is performed on several-hundred- μm -thick single crystal substrates which are expensive. These bulk substrates represent a significant waste of material since only the very last atomic planes are useful to induce epitaxial growth. In principle, an ultimately thin material should be sufficient. Furthermore, as compared with a substrate of several hundred μm thickness, a monoatomic film presents a much higher compliance to accommodate the lattice mismatch with an epilayer.

Among the potential candidates, graphene is a model 2D material that can be produced in large areas from an abundant elemental resource. On the other hand, GaN is one of the most important III-V semiconductors from the point of view of applications, but there is no cheap and well-suited bulk substrate for its epitaxial growth. The combination of epitaxial GaN on graphene is therefore a particularly interesting case to explore.

Several attempts to combine these two materials by epitaxy have been reported^{1,2}. Some of these studies focused on the approach called « remote epitaxy »³, where graphene is grown or transferred onto a single crystal substrate. In these studies, the underlying crystalline substrate is supposed to drive the epitaxy and the main advantage is that the epitaxial layers can later be mechanically separated from the original substrate and transferred to another substrate. Here, we are interested in the situation where the epitaxial relationship is directly and unambiguously dictated by a graphene sheet. A few studies have demonstrated that this is possible: the growth

of vertical nanowires with a well-defined basal orientation has been observed on multilayer graphene, thick enough to exclude a role for the underlying SiC^{4,5} bulk substrate. Moreover, in our past studies, we transferred graphene onto a thick layer of amorphous SiO₂ and we also observed a unique basal alignment of GaN nanowires on graphene⁶. The photoluminescence properties of these nanowires are comparable to that we obtained for GaN nanowires grown on conventional Si (111) substrates⁷. We have also shown that the first GaN seeds on graphene are under tension, which is a further sign of epitaxial growth⁸. Based on these observations, we have suggested a possible epitaxial relationship where three GaN unit cells coincide with four graphene unit cells. This lattice arrangement requires a 3.1 % misfit accommodation⁶. However, the nature of the interactions at the interface remains an open question that we address in the present study. We explore the mechanisms of this unusual epitaxial growth, by plasma-assisted molecular beam epitaxy (PA-MBE). We observe that GaN nucleation does not occur before a long period of exposure to the incident growth species. We seek for surface changes that may occur during this long delay and that could trigger GaN nucleation, using morphological characterization by atomic force microscopy (AFM), chemical analyses by X-ray photoemission spectroscopy (XPS) and structural investigation by scanning tunnelling microscopy (STM). Then, we determine and model the variation of the delay time with the growth parameters. Finally, we test the bond strength at the interface between the two materials by applying mechanical stress to GaN nano-objects with an AFM tip.

Experimental conditions

For the preparation of the substrates, we used a wet process to transfer about 1 cm² of a polycrystalline monolayer of graphene onto a 300-nm-thick amorphous SiO₂ carrier layer obtained by thermal oxidation of an n-type Si (100) substrate. The sample surface therefore

consists of this 1 cm² graphene patch surrounded by SiO₂. The commercial graphene films used for this experiment were grown by chemical vapor deposition (CVD) on a copper foil and present grain sizes of tens of μm. The samples are introduced and outgassed in the MBE system. Then, the substrate temperature is stabilized at the growth temperature, T_g , and the surface is exposed to the beam flux of a Ga effusion cell, ϕ_{Ga} , and to the flux of nitrogen species emitted from a radio-frequency (RF) plasma source, ϕ_N . The Raman spectra of the graphene monolayer at the different stages of this process are reported in the supporting information (Figure S2). Our standard conditions correspond to a Ga flux ϕ_{Ga0} giving a planar GaN growth rate of 0.62 monolayer/s (or 9.6 nm/min), and a N flux ϕ_{N0} corresponding to N/Ga ratio in the vapor phase of 1.1 (the equivalent planar growth rate is 10.5 nm/min) and a growth temperature T_{g0} of 815°C. Under these conditions, we obtain nanowires with a well-defined epitaxial relationship with graphene, as described in our previous studies⁶. The onset of GaN growth is monitored by reflection high-energy electron diffraction (RHEED). Under our standard conditions and from the beginning of the exposure of graphene to the atomic fluxes, it takes about 90 min before GaN-related diffraction spots can be detected (Figure 1b). Before that, a diffuse pattern with no diffraction feature is observed (Figure 1a). After 180 min of exposure to N and Ga fluxes (about twice the previous delay), the RHEED pattern consists of well-defined spots (Figure 1c) corresponding to GaN nanowires of hexagonal crystal structure. Scanning electron microscopy (SEM) images of samples obtained after different exposure times are shown in the bottom row of Figure 1. Very few nanowires have nucleated after 100 min (Figure 1d) but new nanowires rapidly appear afterwards (Figure 1e) until forming a dense array that grows on the graphene patch but not on the surrounding SiO₂ (Figure 1f). The appearance of the first diffraction spots therefore corresponds to the formation of the first GaN seeds on graphene. The period that precedes will be called the incubation time.

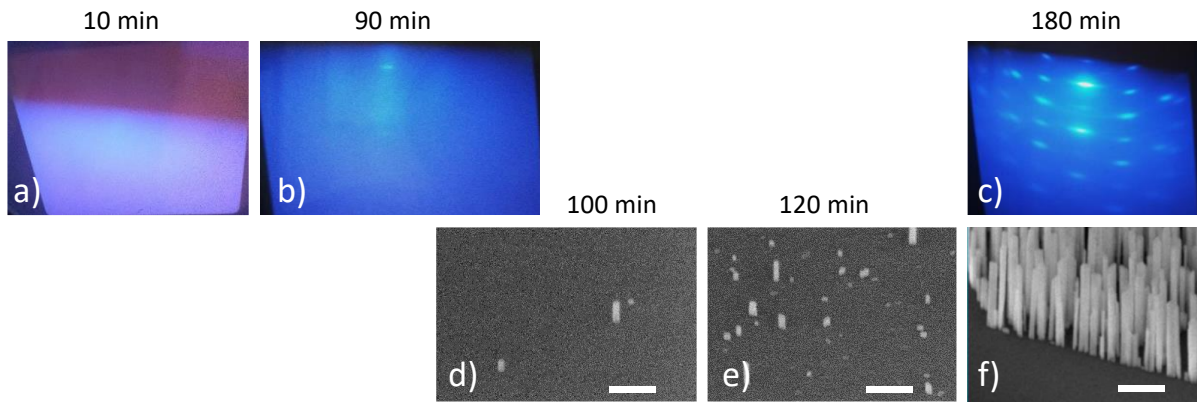


Figure 1. RHEED patterns (a-c) and SEM bird's eye views (d-f) of samples after different times of exposure of a graphene layer to molecular beams of Ga and N in our standard conditions. The times of exposure are indicated above the pictures. f) Nanowire array at the edge of the graphene patch transferred onto SiO_x. Scale bars in (d-f): 200 nm.

Such a time delay before GaN nanowire growth on crystalline Si (111)^{9,10} or on amorphous Al_xO_y/Si and SiN_x/Si substrates^{11,12} has been observed by several authors. It was shown that it can vary between a few minutes and several hours, depending on growth parameters and substrate. These variations were modeled and the origin of the incubation was discussed. In our study, we will address similar questions and clarify what happens during this long incubation period, in the case of growth on graphene.

A priori, the low reactivity of graphene is not favorable to the nucleation of GaN. However, the nitrogen plasma generates neutral and ionised active species that can react with the exposed surface. In particular, it has been shown that N doping can result from the exposure of a graphene layer to a N plasma¹³. To check the impact of the N plasma exposure on the graphene in our conditions, we study two series of samples by AFM and XPS. The AFM measurements were performed using a Bruker ICON instrument in a tapping configuration. The XPS measurements used a non-monochromatic Al-K α (1486.6 eV) source (XR50) operating at 200 W and a PHOIBOS 100 hemispherical electron analyser with 5 Channeltrons (from SPECS). The angles between sample surface normal and (i) X-ray source or (ii) spectrometer were 28°

and 24.5°, respectively. Prior to XPS measurement, the samples were annealed during 30 min at 400°C under a residual pressure of $\sim 10^{-7}$ mbar. During the acquisitions, the analysis chamber pressure was maintained below 10^{-8} mbar. For each sample, the high-resolution spectra of C1s and N1s (with Si2p, not shown) were recorded with a pass energy of 15 eV and a step width of 0.1 eV. The peak background was modeled by a Shirley function and the resulting peak profile was fitted using Gaussian (70%) - Lorentzian (30%) contributions. All the binding energies shifts due to surface charging effect were corrected assuming the Si2p main line centroid related to SiO₂ is at 103.3 eV (for the native oxide at wafer surface).

Results

In a first series, samples are exposed to the N plasma alone while in the second, samples are exposed to the N plasma and to the Ga flux simultaneously. For each series, the time of exposure is varied. Figure 2 presents AFM images of these samples and includes that of a reference graphene layer (Figure 2a) which was not exposed. This as-transferred sample does not show any peculiar feature and the root mean square (RMS) surface roughness is 0.15 nm. The roughness increases with the N exposure time from 0.17 nm (30 min exposure) to 0.37 nm (90 min exposure). At 60 and 90 min, pinholes of 5 to 12 nm in diameter and 1.2 nm in depth become visible in the graphene layer (Figure 2b). The depth of the holes is less than the step height measured at the edge of the graphene patch (see supporting information, Figure S3). We can therefore rule out the possibility that the holes in the graphene extend into the SiO₂. For the samples exposed to Ga and N fluxes simultaneously, after 10 min, no clear feature appears but the RMS roughness increases slightly. After 60 min exposure to both species, unlike exposure to N plasma alone, pinholes are not observed but instead, small islands of about 10 nm diameter and 0.3 nm height appear.

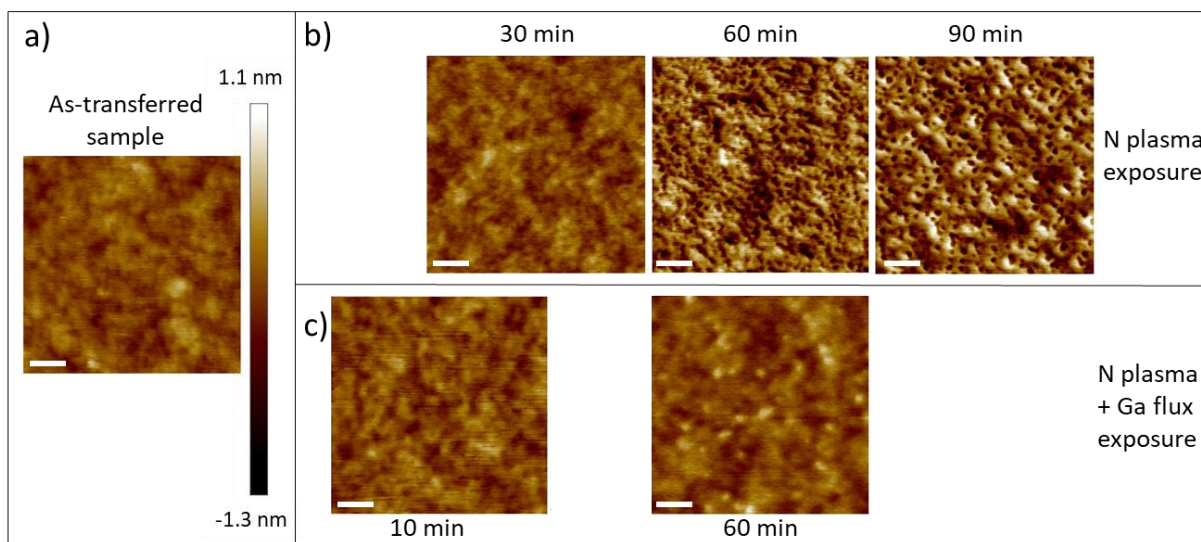


Figure 2. Atomic force microscopy images of graphene layers; a) as-transferred sample with no exposure; b) samples exposed to N plasma for 30, 60 and 90 min; c) samples exposed to N plasma and Ga flux simultaneously for 10 and 60 min. Scale bars: 50 nm. Z color scale is common to all images.

We selected three of these samples for XPS analyses: the as-transferred sample, the sample exposed for 90 min to N plasma and the sample exposed to N plasma and Ga flux for 60 min. Figure 3 shows the spectra for C1s and N1s core levels. We first discuss the C1s spectra (Figure 3a-c). As expected, the C-C sp^2 peak dominates the spectrum of the as-transferred sample whereas a strong contribution of C-N bonds appears for the sample exposed to N radicals alone. Similarly, the spectrum of the sample exposed to N and Ga shows a strong signal related to C-N bonds. This contribution, observed in the two samples after exposure but not in the as-transferred sample, proves that N atoms become chemically bonded to the graphene lattice during the plasma exposure. The other contributions are discussed in the supporting information. Several possible N incorporation sites into graphene are reported in the literature: graphitic in substitution of a carbon atom, pyridinic and pyrrolic in association with neighboring vacancies (Figure 3d). They can be identified by examining the N1s spectra^{14,15,16,17} (Figure 3e-f).

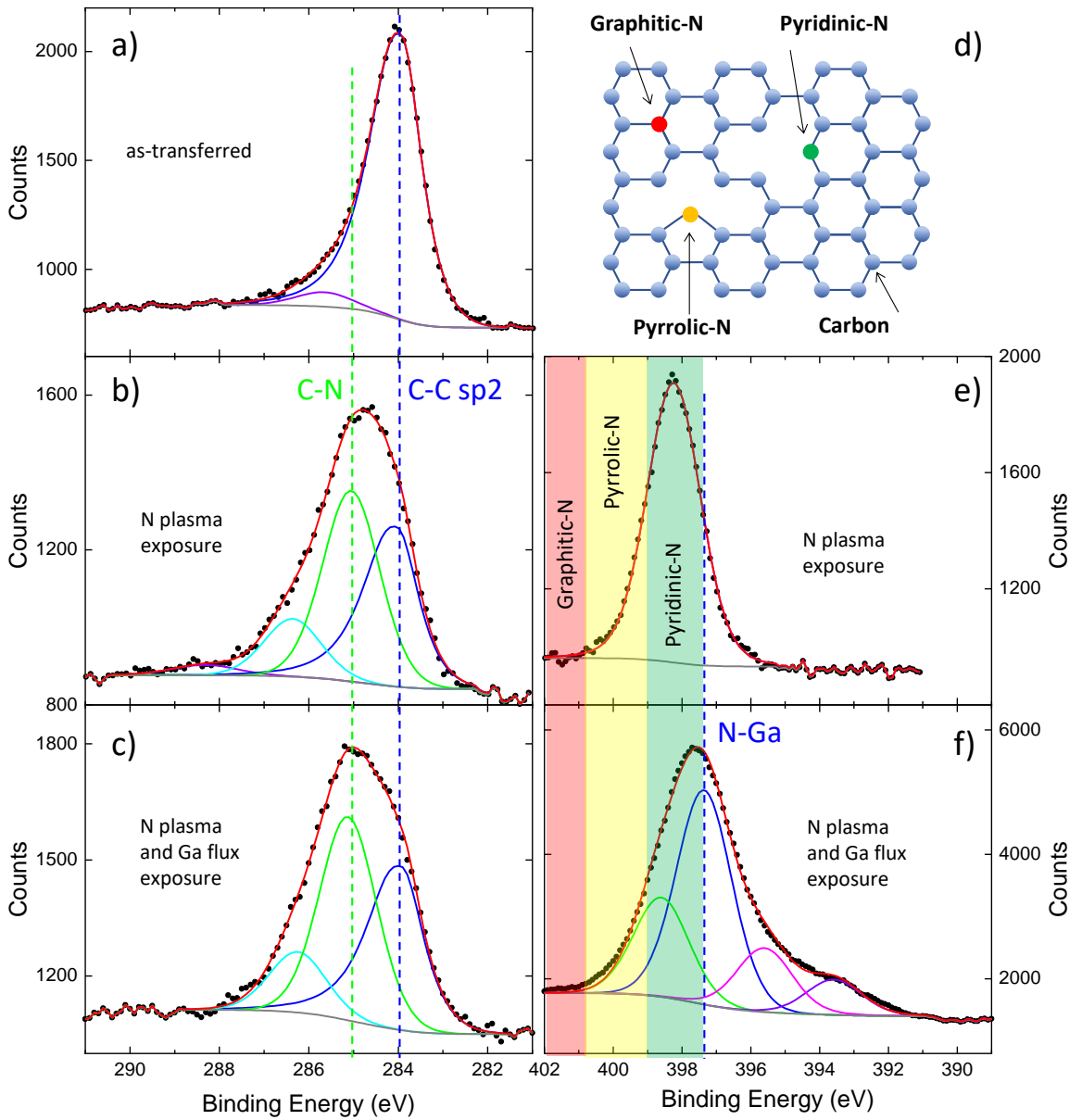


Figure 3: XPS spectra of C1s (a, b, c) and N1s (e, f) core levels for a) as-transferred graphene layer; b) and e) graphene layer exposed to N plasma for 90 min; c) and f) graphene layer exposed to N plasma and Ga flux for 60 min. The dots correspond to the experimental data and the red line is a fit based on multiple contributions detailed in the supporting information. The vertical dotted lines indicate the peak positions of the main contributions, C-C and C-N for a) b) and c), N-Ga for e) and f). d) Schematics of possible incorporation sites of N into a graphene

lattice. The expected positions of the XPS signatures for the three possible N incorporation sites are shown as coloured rectangles in e) and f), red for graphitic, yellow for pyrrolic and green for pyridinic.

Figure 3e shows that in the sample exposed to N plasma alone, the majority of the nitrogen atoms were incorporated in pyridinic sites. Note that these pyridinic sites might be available at the periphery of the pinholes that we observed by AFM. Indeed, as shown in Figure 3d, a pyridinic N is bonded to two carbon atoms and is located near vacancies in the graphene lattice. For the sample exposed to N and Ga, the N1s spectrum shows a broader peak (Figure 3f) which contains the contributions of pyridinic nitrogen but also three other components corresponding to N bonded to Ga (397.4 eV)¹⁸ and to Ga LMN Auger transition (393,6 and 395,6eV). This indicates that GaN seeds are present on this sample. They probably correspond to the small islands observed in the AFM image of its surface (Figure 2). We note that neither sample shows a significant signal around the expected binding energies for graphitic or pyrrolic nitrogen.

Additional characterisations were carried out by STM on two samples: the as-transferred graphene and the graphene exposed for 30 min to N plasma (the electrical conductivity of the other graphene samples degraded significantly upon exposure to the fluxes, making their STM analysis impossible). The samples were outgassed at 570°C for one hour in a preparation chamber. The STM measurements were performed at 77 K with a tunnelling current of 1 nA and a voltage of 20 mV. The image of the reference graphene indicates that the transfer process was clean (Figure 4a): the hexagonal lattice of the graphene is clearly visible, with no sign of residual contamination, and the corrugations are similar to the intrinsic ripples reported for suspended graphene¹⁹. The image of the sample exposed to N plasma for 30 min (Figure 4b) is very different. Strong modifications of the graphene lattice are evidenced. The Fourier transform of the image reveals a ($\sqrt{3} \times \sqrt{3}$) super-periodicity, rotated by 30° from the graphene lattice. Such pattern is associated with interference arising from intervalley scattering induced

by point defects²⁰. We therefore conclude that 30 min of exposure to N plasma is sufficient to induce significant changes to the graphene layer.

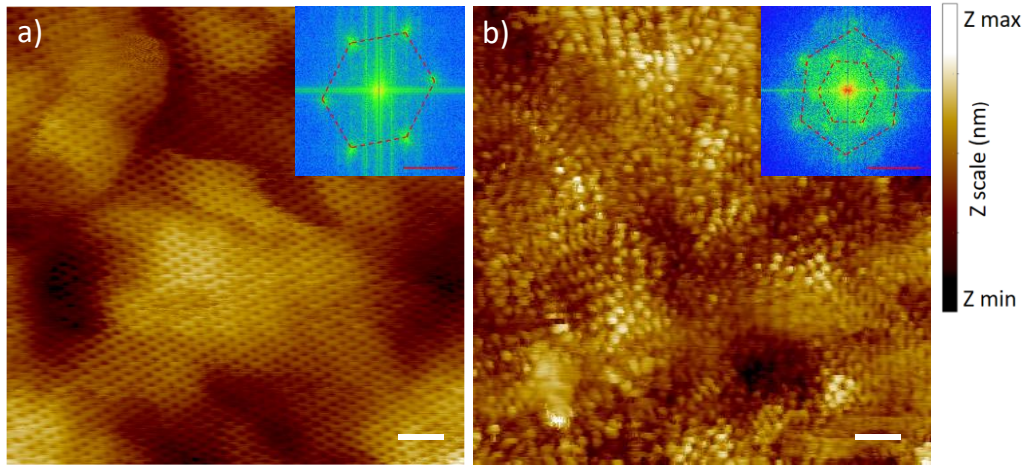


Figure 4: Scanning tunnelling microscopy images of the as-transferred graphene sample (a) and of the graphene sample exposed for 30 min to N plasma (b). White scale bars are 1 nm and Z_{max} is 0.35 nm and 0.45 nm, for a and b, respectively. Fast Fourier transforms are shown in the insets. Red scale bars indicate the reciprocal lattice vector norm (29.5 nm^{-1}).

All the above observations lead us to propose a scenario for the nucleation of GaN on graphene. Exposure to energetic N plasma species damages the graphene lattice to the extent of producing pinholes on the edges of which N atoms can attach in pyridinic sites. These pyridinic N atoms are anchor points for the first GaN bonds, from which GaN islands are formed that later evolve into nanowires. In this scenario, the incubation time would include the following steps: the creation of vacancies and then pinholes in the graphene lattice, the attachment of N atoms to the pinhole edges, the formation of critical GaN nuclei bonded to these first incorporated nitrogen atoms and the beginning of the seed extension until sufficient material is deposited to be detected as a diffraction spot in the RHEED pattern. We exclude the possibility that GaN nuclei anchor to SiO_2 inside the pinholes because growth is highly selective at T_{g0} . Moreover, we cannot see any pinhole expansion when both Ga and N fluxes are provided, which probably indicates that these pinholes remain very tiny before GaN islands appear.

To further analyse the origin of the incubation time, τ_i , and to identify strategies to reduce it, we first studied its variations with the growth temperature, T_g , using our standard Ga and N fluxes, ϕ_{Ga0} and ϕ_{N0} . τ_i is measured by observing the RHEED pattern and detecting an increase of intensity at the expected location of the first GaN-related spot. The incubation shortens rapidly when the growth temperature is decreased (Figure 5). But, at the same time, the growth selectivity deteriorates: at reduced temperature, GaN nanowires start to nucleate on the SiO₂ surface surrounding the graphene area²¹ (see supporting information). Below 800°C, the selectivity is even reversed: the first GaN NWs nucleate on SiO₂ before appearing on the graphene. Note that this introduces a large uncertainty in our determination of the incubation time in this temperature range. Indeed, at 785°C, the initial GaN RHEED signal reveals the nucleation of GaN on SiO₂ and not on graphene. To estimate the incubation time on graphene at this temperature, SEM observation after a limited growth time following the onset of nucleation on SiO₂ is necessary to check the presence of nanowires on the graphene area. This was done for 20 and 50 min of growth after an observed incubation time on SiO₂ of 10 min. We could observe nanowires on graphene for 50 min but not for 20 min, hence the error bar at 785°C in Figure 5. The value of τ_i which is tentatively plotted for this temperature is deduced from the comparison of the average lengths of the nanowires on graphene and SiO₂, assuming constant and equal nanowire growth rates after nucleation on each of these two materials.

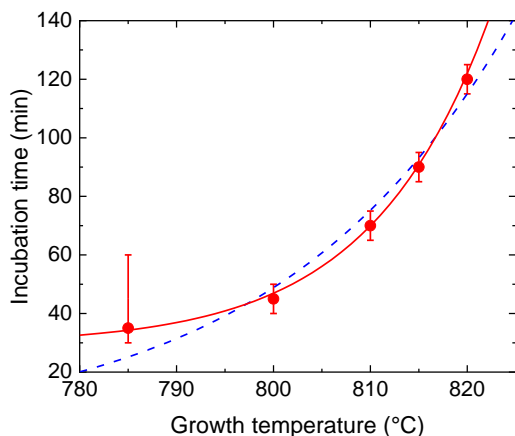


Figure 5. Dependence of the incubation time upon growth temperature. Experimental data (dots) fitted with an Arrhenius law (dashed line) or with an Arrhenius law plus a damage time τ_{d0} (solid line).

To describe our experimental data, we first follow other authors^{11,12} and simply use an Arrhenius expression:

$$\tau_i = A \exp\left(-\frac{E_N}{k_B T}\right) \quad (1)$$

where A is a parameter which depends on the incoming fluxes ϕ_{Ga} and ϕ_N , E_N an activation energy and k_B the Boltzmann constant. While this expression describes our results reasonably well (dashed line in Figure 5), a better fit (solid line in Figure 5) is obtained by adding a temperature-independent term τ_d to the previous expression:

$$\tau_i = \tau_d + A' \exp\left(-\frac{E_N}{k_B T}\right) \quad (2)$$

In our tentative scenario, τ_d would correspond to the time needed to create anchor points in the graphene lattice, while the Arrhenius term would describe the subsequent nucleation process itself. The best fit results in a nucleation barrier E_N of 8.5 eV. This value lies between those reported for the nucleation of GaN nanowires on amorphous Al_xO_y (6.0 eV) and on SiN_x (10.2 eV)¹¹. τ_d is determined at 29.6 min for this series of samples. The AFM, XPS and STM studies clearly showed that the exposure to N plasma was responsible for an alteration of graphene. At 30 min, the AFM image in Figure 2 does not yet show clear evolution of the graphene surface under plasma exposure, but the STM analysis (Figure 4b) proves that the graphene lattice has been significantly modified. Our value of τ_d is therefore consistent with the time necessary to produce the first modifications of the graphene. In the following, τ_d is referred to as the *damage time*. Once τ_d has elapsed, GaN nucleation becomes possible but additional time, described by the second term on the right-hand side of Equation (2), is required to overcome the nucleation barrier. This nucleation barrier reflects the activation of different microscopic processes involved in the formation of GaN islands on the damaged graphene. Some of these processes are necessary to form a stable nucleus (adsorption, surface diffusion of adatoms, bonding to

nucleation centers) but others act against this formation (desorption of adatoms, desorption from the nucleus). Since the incubation time increases with temperature, Figure 5 mainly highlights the activation of desorption mechanisms. As for the nucleation centers, they are most likely associated to the pyridinic N atoms incorporated into the graphene lattice.

Then, we investigated the effect of the Ga flux for three different N fluxes at our standard growth temperature of 815°C, T_{g0} . The results are summarized in Figure 6. Increasing ϕ_{Ga} or ϕ_N results in a reduced incubation time. This is expected as higher ϕ_{Ga} or ϕ_N lead to a higher density of surface adatoms, making GaN nucleation more likely. We first tentatively fit our experimental data with the following power law:

$$\tau_i = \frac{B}{\phi_{Ga}^p \phi_N^q} \quad (3)$$

where B is a parameter containing the substrate temperature dependence and p and q are positive exponents related to the microscopic details of the nucleation process. This expression has been used for the nucleation of GaN nanowires on various substrates. p was found close to 1 in the case of GaN nanowires grown on amorphous Al_xO_y ¹² and it was interpreted as related to a heterogeneous nucleation mechanism driven by a high density of nucleation centers²². For a SiN_x surface, or more generally a Si surface exposed to N, values of p between 1.5 and 2.1 were reported¹⁰⁻¹². In the latter cases, the exponent was related to the size of the critical nucleus, p being, in a first approximation, the number of Ga atoms constituting it²³.

In our case, the best fit using Equation 3 is obtained with $p = 1.1$ and $q = 1.7$. It correctly describes the general trends but does not reproduce the asymptotic behaviour of the incubation time at high Ga fluxes (see Figure S9a in supporting information). Indeed, the experimental data hint at the existence of an incompressible time and reinforce the idea that a damage period precedes the nucleation process. Hence, as for the description of the temperature dependence,

we add in the expression of τ_i a time τ_d corresponding to the initial modification of the graphene surface:

$$\tau_i = \tau_d + \frac{B'}{\phi_{Ga}^p \phi_N^q} \quad (4)$$

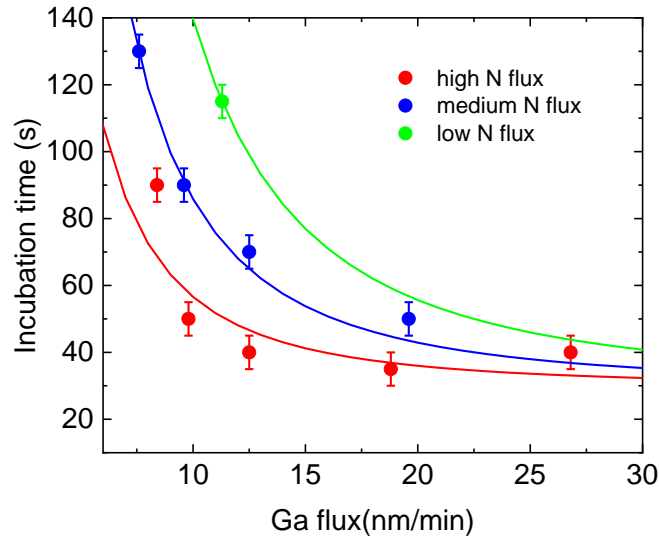


Figure 6. Dependence of the incubation time with Ga flux, for high (red plots), medium (blue plots) and low (green plots) N flux, at $T=815^\circ\text{C}$. Full circles: experimental data. Lines: power-law fits with the addition of a damage time τ_d .

We take $\tau_d = 29.6$ min, the value determined with the previous series of samples. To be fully consistent with the fit of this temperature series (Equation (2)), we take B' such that it satisfies condition:

$$\frac{B'}{\phi_{Ga0}^p \phi_{N0}^q} = A' \exp\left(-\frac{E_N}{k_B T_{g0}}\right) \quad (5)$$

Equation (5) imposes the expressions of τ_i in Equations (2) and (4) to be equal for our standard growth conditions T_{g0} , ϕ_{Ga0} and ϕ_{N0} . With these constraints, Equation (4) becomes:

$$\tau_i = \tau_d + A' \left(\frac{\phi_{Ga0}}{\phi_{Ga}} \right)^p \left(\frac{\phi_{N0}}{\phi_N} \right)^q \exp \left(- \frac{E_N}{k_B T_{g0}} \right) \quad (6)$$

A' and E_N being determined by the previous fit, Equation (6) has only two adjustable parameters, namely exponents p and q . This expression leads to a better agreement with the series of experiments at variable ϕ_{Ga} and ϕ_N (Figure 6). The best fit is now obtained with $p = 2.1$ and $q = 3.0$. These values are quite comparable to those reported for a SiN_x surface and suggest a critical nucleus composed of a few atoms, typically two Ga and three N atoms. Since the N plasma is the source of the damage, one could assume that τ_d is inversely proportional to the nitrogen flux ϕ_N . The best fit obtained with this assumption is also satisfying (see Figure S9c of supporting material) and leads to $p=1.9$ and $q=2.0$.

The decomposition of the incubation time into two components is therefore further supported by these additional experimental data. As evidenced by our AFM and STM studies, the energetic N species that are emitted from the plasma source alter the graphene surface. In the absence of Ga flux, the alteration is first manifested by interference patterns observed by STM and arising from scattering of electrons by local defects. At longer N exposure, the AFM reveals the formation of pinholes. The XPS analysis indicates that the exposure to N alone or to both N and Ga results in the incorporation of pyridinic N in the graphene lattice. These pyridinic N atoms possess a lone pair of electrons, a favorable configuration to bind Ga atoms in turn. Moreover, compared to highly volatile N adatoms, the residence time of C-bound N atoms at the surface is quasi-infinite. Thus, the first GaN bond can be formed much more easily at these anchor points. The agglomeration of a few GaN pairs is then sufficient to reach the critical nucleus size and to promote its evolution into a nanowire. In our scenario, the damage time τ_d would correspond to the mechanisms leading to the incorporation of pyridinic N into the graphene lattice. The second part of the incubation time would describe the time for binding Ga to the pyridinic N atoms and for GaN nuclei to form and grow until a RHEED signal can be

detected. This second part is highly dependent on the growth conditions, namely temperature and incoming fluxes, which determine the supersaturation of the surface adatoms.

Finally, in order to confirm the presence of chemical bonds between the GaN nanowires and their graphene substrate, we applied mechanical stress to these nano-objects with an AFM tip. Journot and coworkers performed such a test on GaN tetrahedra grown on graphene by metalorganic vapor phase epitaxy (MOVPE)²⁴. Initially, their tetrahedra presented a well-defined in-plane orientation on the graphene lattice. By simply pushing these nanocrystals with an AFM tip, they were able to move them. With this experiment, they evidenced that the interaction between the grown crystal and the graphene substrate is weak. Their work illustrated a genuine example of van der Waals epitaxy, *i.e.* without strong chemical bonds at the interface between the two crystals.

To fairly compare the behaviour of our nanowires to their result, we performed a MOVPE growth on a graphene sample prepared as for our PA-MBE samples. Among other nano-objects, we obtained GaN tetrahedra as in Journot *et al.*'s experiment. Then, we tried to reproduce their result by pushing a tetrahedron with an AFM tip of 46 N/m stiffness. The experiment consists of a first scan in tapping mode to image the initial position of the tetrahedron (Figure 7a), a second scan in contact mode along a single line (arrow in Figure 7) during which the nano-object is laterally stressed by the tip and a third scan in tapping mode to image the new position of the nano-object (Figure 7b). As can be seen, the tetrahedron was translated and slightly rotated by the tip. Dividing the maximum of the friction force recorded during the scan (see supporting information) by the contact area of the tetrahedron on graphene, we obtain a value of $1.1 \mu\text{N}/\mu\text{m}^2$.

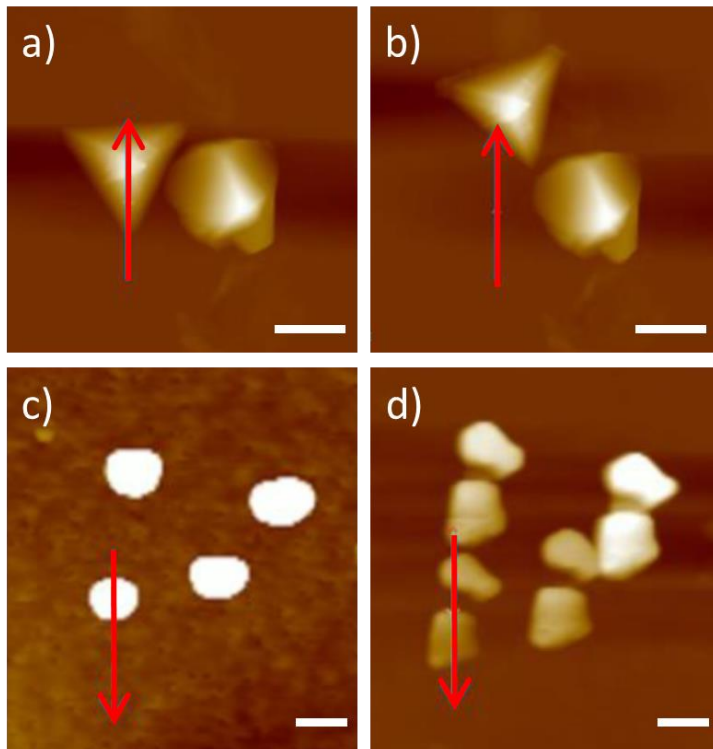


Figure 7. AFM images before (a, c) and after (b, d) applying a stress on a GaN tetrahedron grown by MOVPE (a, b) and a GaN nanowire grown by PA-MBE (c, d). The stress is applied by scanning the tip in contact mode along the red arrows. The tetrahedron is displaced (a, b). The nanowire cannot be moved and the tip is damaged during the stress test. Scale bar: 500 nm in (a,b), 100 nm in (c,d)

The same test was performed on a nanowire grown by PA-MBE at 815°C (Figure 7c). Using a comparable force, the initial position of the nanowire remained unchanged after the scan of the tip in contact mode. Then, a stronger force was applied and the tip was damaged during this second test. Indeed, the image of the nanowire after the test (Figure 7d) is deformed and duplicated. The same occurs for three neighbouring nanowires. This evidences that the tip has split into two parts, resulting in a degraded and two-fold image of the objects. However, the important information is that the probed nanowire did not move. Indeed, the relative positions of the four nanowires remain unchanged. During this test, the friction force per nanowire unit area was $1100 \mu\text{N}/\mu\text{m}^2$, i.e. 10^3 stronger than for the test which displaced the tetrahedron.

This experiment highlights the different nature of interactions at the tetrahedron/graphene and nanowire/graphene interfaces. Since the tetrahedra were obtained by MOCVD and the nanowires by MBE, the Ga and N precursors of these two growth techniques may interact differently with the graphene substrate at the early stage of the growth experiments. More particularly, the NH_3 gas flow used in MOVPE is certainly less aggressive for the graphene

layer than the N species generated by the MBE plasma cell. While the tetrahedra probably form on unmodified graphene with van der Waals adhesion forces, a much stronger interfacial binding is revealed for the nanowires. This binding is strong enough to maintain a GaN nanowire at its initial position during the stress test. This is again consistent with the existence of some C-N chemical bonds at the nanowire/graphene interface, which inevitably implies graphene modifications.

Conclusion

Our study focused on the origin of the incubation time that precedes the PA-MBE growth of GaN nanostructures on graphene. We tried to identify what triggers nucleation. We show that after several tens of minutes of exposure to N plasma, in our conditions, graphene is modified and N incorporates as pyridinic atoms. We suggest that these pyridinic-N atoms, identified by XPS, are the starting points for the nucleation of GaN nanostructures on graphene. The presence of covalent C-N bonds as anchor points for the GaN nanowires is also supported by the strong adhesion between the two crystals. This adhesion, probed by AFM, is much stronger than a van der Waals interaction. We also investigated the dependence of the incubation time upon temperature and N and Ga fluxes. The experimental results are very well described with a model considering two time-components. The first corresponds to a damage time, which leads to the graphene modification and to the incorporation of pyridinic N. The second is the time necessary to overcome a nucleation barrier and form critical GaN nuclei. We fit the whole experimental data with a single set of adjustable parameters: a common prefactor, a nucleation barrier of 8.5 eV, a critical nucleus composed of two to three (Ga,N) pairs and a damage time of the order of 30 min, depending on N flux. Our study suggests different strategies to reduce the incubation time, which appears necessary to make graphene an attractive substrate for GaN. One could apply a pre-treatment to graphene to create nucleation centers prior to growth. We propose

focused ion beam as a possible technology for this treatment. The damage time component would be removed from the incubation time. Then, to get faster nucleation, one should, as expected, use high Ga and N fluxes and low growth temperature, keeping in mind that the selectivity of the deposition on graphene (with respect to SiO₂) is lost if the temperature is too low.

Corresponding Author

*Jean-Christophe Harmand, jean-christophe.harmand@c2n.upsaclay.fr

Present Addresses

Camille Barbier is presently at Tyndall National Institute, University College Cork, Lee Maltings, Dyke Parade, Cork, Ireland.

Author Contributions

The manuscript was written through contributions of all authors. All authors have given approval to the final version of the manuscript.

Funding sources

We received funding from LABEX GANEX, from ANR, the French National Research Agency, within the project FLAGG (grant ANR-21-CE24-0017-01) and from the French RENATECH network.

Supporting information

Additional experimental details on growth selectivity, AFM profiles, analysis of XPS spectra, fit of the incubation time dependence with the fluxes and stress tests with the AFM tip. Raman spectra of representative samples are also provided (DOCX).

ACKNOWLEDGMENT

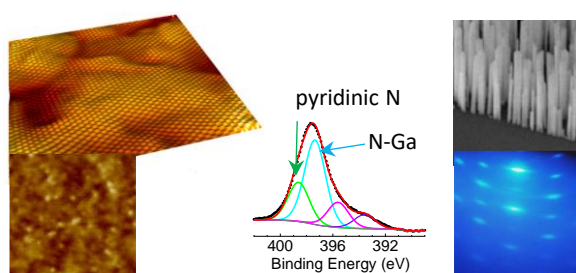
This work was partly performed in the C2N nanotechnology platform. We acknowledge the engineers of this platform for their assistance with specific technological steps and for training our students.

For Table of Contents Use Only

What triggers epitaxial growth of GaN on graphene?

Camille Barbier, Ludovic Largeau, Noëlle Gogneau, Laurent Travers, Christophe David, Ali Madouri, Dyhia Tamsaout, Jean-Christophe Girard, Guillemin Rodary, Hervé Montigaud, Christophe Durand, Maria Tchernycheva, Frank Glas, Jean-Christophe Harmand

TOC graphic



Synopsis

This work explores how a graphene monolayer is modified before nucleation and growth of GaN nanowires by plasma-assisted molecular beam epitaxy becomes possible on it. It is shown that the graphene is damaged by the N plasma and that the N atoms become incorporated into pyridine sites before the first GaN bonds are formed. It is thought that the pyridinic N atoms are the anchor points for this GaN epitaxy on graphene, which is not of the van der Waals type.

REFERENCES

- ¹ Kim, J.; Bayram, C.; Park, H.; Cheng, C. W.; Dimitrakopoulos, C.; Ott, J. A.; Reuter, K. B.; Bedell, S. W.; Sadana, D. K. Principle of direct van der Waals epitaxy of single-crystalline films on epitaxial graphene. *Nature Communications* **2014**, *5*. DOI: 10.1038/ncomms5836.
- ² Kobayashi, Y.; Kumakura, K.; Akasaka, T.; Makimoto, T. Layered boron nitride as a release layer for mechanical transfer of GaN-based devices. *Nature* **2012**, *484* (7393), 223-227. DOI: 10.1038/nature10970.
- ³ Kim, Y.; Cruz, S. S.; Lee, K.; Alawode, B. O.; Choi, C.; Song, Y.; Johnson, J. M.; Heidelberger, C.; Kong, W.; Choi, S.; et al. Remote epitaxy through graphene enables two-dimensional material-based layer transfer. *Nature* **2017**, *544* (7650), 340. DOI: 10.1038/nature22053.
- ⁴ Fernandez-Garrido, S.; Ramsteiner, M.; Gao, G. H.; Galves, L. A.; Sharma, B.; Corfdir, P.; Calabrese, G.; Schiaber, Z. D.; Pfuller, C.; Trampert, A.; et al. Molecular Beam Epitaxy of GaN Nanowires on Epitaxial Graphene. *Nano Letters* **2017**, *17* (9), 5213-5221. DOI: 10.1021/acs.nanolett.7b01196.
- ⁵ Munshi, A. M.; Dheeraj, D. L.; Fauske, V. T.; Kim, D. C.; van Helvoort, A. T. J.; Fimland, B. O.; Weman, H. Vertically Aligned GaAs Nanowires on Graphite and Few-Layer Graphene: Generic Model and Epitaxial Growth. *Nano Letters* **2012**, *12* (9), 4570-4576. DOI: 10.1021/nl3018115.
- ⁶ Kumaresan, V.; Largeau, L.; Madouri, A.; Glas, F.; Zhang, H. Z.; Oehler, F.; Cavanna, A.; Babichev, A.; Travers, L.; Gogneau, N.; et al. Epitaxy of GaN Nanowires on Graphene. *Nano Letters* **2016**, *16* (8), 4895-4902. DOI: 10.1021/acs.nanolett.6b01453.
- ⁷ Kumaresan, V.; Largeau, L.; Oehler, F.; Zhang, H.; Mauguin, O.; Glas, F.; Gogneau, N.; Tchernycheva, M.; Harmand, J.-C. *Nanotechnology* **2016**, *27*, 135602. DOI: 10.1088/0957-4484/27/13/135602
- ⁸ Barbier, C.; Zhou, T.; Renaud, G.; Geaymond, O.; Le Fevre, P.; Glas, F.; Madouri, A.; Cavanna, A.; Travers, L.; Morassi, M.; et al. In Situ X-ray Diffraction Study of GaN Nucleation on Transferred Graphene. *Crystal Growth & Design* **2020**, *20* (6), 4013-4019. DOI: 10.1021/acs.cgd.0c00306.
- ⁹ Zettler, J. K.; Hauswald, C.; Corfdir, P.; Musolino, M.; Geelhaar, L.; Riechert, H.; Brandt, O.; Fernandez-Garrido, S. High-Temperature Growth of GaN Nanowires by Molecular Beam Epitaxy: Toward the Material Quality of Bulk GaN. *Crystal Growth & Design* **2015**, *15* (8), 4104-4109. DOI: 10.1021/acs.cgd.5b00690.
- ¹⁰ Fernandez-Garrido, S.; Zettler, J. K.; Geelhaar, L.; Brandt, O. Monitoring the Formation of Nanowires by Line-of-Sight Quadrupole Mass Spectrometry: A Comprehensive Description of the Temporal Evolution of GaN Nanowire Ensembles. *Nano Letters* **2015**, *15* (3), 1930-1937. DOI: 10.1021/nl504778s.
- ¹¹ Consonni, V.; Trampert, A.; Geelhaar, L.; Riechert, H. Physical origin of the incubation time of self-induced GaN nanowires. *Applied Physics Letters* **2011**, *99* (3). DOI: 10.1063/1.3610964.
- ¹² Sobanska, M.; Dubrovskii, V. G.; Tchutchulashvili, G.; Klosek, K.; Zytkeiwicz, Z. R. Analysis of Incubation Times for the Self-Induced Formation of GaN Nanowires: Influence of the Substrate on the Nucleation Mechanism. *Crystal Growth & Design* **2016**, *16* (12), 7205-7211. DOI: 10.1021/acs.cgd.6b01396.
- ¹³ Joucken, F.; Tison, Y.; Lagoute, J.; Dumont, J.; Cabosart, D.; Zheng, B.; Repain, V.; Chacon, C.; Girard, Y.; Botello-Mendez, A. R.; et al. Localized state and charge transfer in nitrogen-doped graphene. *Physical Review B* **2012**, *85* (16). DOI: 10.1103/PhysRevB.85.161408.
- ¹⁴ Xie, W.; Weng, L.T.; Ng, K.M.; Chan, C.K.; Chan, C.M. Clean graphene surface through high temperature annealing. *Carbon* **2015**, *94*, 740-748. DOI: 10.1016/j.carbon.2015.07.046.

-
- ¹⁵ Matsoso, B.J.; Ranganathan, K.; Mutuma, B.K.; Lerotholi, T.; Jones, G.; Coville, N.J. Time-dependent evolution of the nitrogen configurations in N-doped graphene films, *RSC Advances* **2016**, *6*, 106914–106920. DOI: 10.1039/c6ra24094a.
- ¹⁶ Wang, H.; Maiyalagan, T.; Wang, X. Review on Recent Progress in Nitrogen-Doped Graphene: Synthesis, Characterization, and Its Potential Applications. *ACS Catalysis* **2012**, *2*, 5, 781–794. DOI : 10.1021/cs200652y
- ¹⁷ Lazar, P.; Mach, R.; Otyepka, M. Spectroscopic Fingerprints of Graphitic, Pyrrolic, Pyridinic, and Chemisorbed Nitrogen in N-Doped Graphene. *Journal of Physical Chemistry C* **2019**, *123* (16), 10695-10702. DOI: 10.1021/acs.jpcc.9b02163.
- ¹⁸ Widstrand, S.M.; Magnusson, K.O.; Johansson, L.S.O.; Moons, E.; Gurnett, M.; Oshima, M. Core-Level Photoemission From Stoichiometric GaN(0001)-1×1. *Materials Research Society Internet Journal of Nitride Semiconductor Research* **2005**, *10*, E1. DOI:10.1557/S1092578300000521
- ¹⁹ Meyer, J.; Geim, A.; Katsnelson, M.; Novoselov, K. S.; Booth, T. J.; Roth, S. The structure of suspended graphene sheets. *Nature* **2007**, *446*, 60–63. DOI: 10.1038/nature05545
- ²⁰ Yan, H.; Liu, C. C.; Bai, K. K.; Wang, X. J.; Liu, M. X.; Yan, W.; Meng, L.; Zhang, Y. F.; Liu, Z. F.; Dou, R. F.; Nie, J. C.; Yao, Y.; He, L. Electronic structures of graphene layers on a metal foil: The effect of atomic-scale defects. *Applied Physics Letters* **2013**, *103*, 143120. DOI: 10.1063/1.4824206.
- ²¹ Mancini, L.; Morassi, M.; Sinito, C.; Brandt, O.; Geelhaar, L.; Song, H. G.; Cho, Y. H.; Guan, N.; Cavanna, A.; Njeim, J.; et al. Optical properties of GaN nanowires grown on chemical vapor deposited-graphene. *Nanotechnology* **2019**, *30* (21). DOI: 10.1088/1361-6528/ab0570.
- ²² Dubrovskii, V. G. Incubation time of heterogeneous growth of islands in the mode of incomplete condensation. *Technical Physics Letters* **2016**, *42* (11), 1103-1106. DOI: 10.1134/s1063785016110158.
- ²³ Venables, J.A.; Spiller, G. D. T.; Hanbucken, M. Nucleation and growth of thin films. *Reports on Progress in Physics* **1984**, *47* (4), 399. DOI 10.1088/0034-4885/47/4/002
- ²⁴ Journot, T.; Okuno, H.; Mollard, N.; Michon, A.; Dagher, R.; Gergaud, P.; Dijon, J.; Kolobov, A. V.; Hyot, B. Remote epitaxy using graphene enables growth of stress-free GaN. *Nanotechnology* **2019**, *30* (50). DOI: 10.1088/1361-6528/ab4501.